



ISTITUTO NAZIONALE DI RICERCA METROLOGICA Repository Istituzionale

Determination of the association constant between the B domain of protein A and the Fc region of IgG

This is the author's submitted version of the contribution published as:

Original

Determination of the association constant between the B domain of protein A and the Fc region of IgG / Ansalone, P. - In: SURFACE AND INTERFACE ANALYSIS. - ISSN 1096-9918. - 46:10-11(2014), pp. 689-692. [10.1002/sia.5500]

Availability:

This version is available at: 11696/65559 since: 2021-03-09T22:00:04Z

Publisher:

Wiley Online Library

Published

DOI:10.1002/sia.5500

Terms of use:

This article is made available under terms and conditions as specified in the corresponding bibliographic description in the repository

Publisher copyright

WILEY

This article may be used for non-commercial purposes in accordance with Wiley Terms and Conditions for Use of Self-Archived Versions

(Article begins on next page)

Determination of the association constant between the B domain of protein A and the Fc region of IgG

P. Ansalone

Department of Electromagnetism, Istituto Nazionale di Ricerca Metrologica (INRIM), Strada delle Cacce 91, 10135, Torino, Italy

The aim of this work is the numerical modelling of the binding mechanism between the Fc region of human IgG interacting with the B domain of Staphylococcal protein A (SpA). The comprehension of the involved kinetics is of noticeable impact for immunosensor diagnostic applications and consequently contributes to increase the sensitivity and efficiency of such devices based on the immobilization of antibodies on biosensor surface. Brownian dynamics methodology is applied to simulate the Fc-SpA encounter. Then, the association rates k_{on} and k_{off} are estimated from the analysis of the diffusional motion between the Fc region and the B domain of SpA combined with continuum electrostatic calculations. Therefore, the association constant K_a between Fc and SpA is calculated. The behaviour of K_a is analysed taking into account the relative distance between SpA and the Fc fragments. The analyses also include the effects on the binding affinity between SpA and Fc due to the variation of the solvent ionic strength and pH values. The association rates and their analyses are presented and discussed showing that the binding mechanism between the SpA and the Fc fragments is enhanced by the nonpolar interaction, while dissociation is driven by the electrostatic repulsion that occurs at relatively low pH. The numerical estimation of the association constant will support the definition of robust protocols for the detection of antibodies via protein A.

Keywords: biosensor; binding; 1FC2; antibody; association constant and Brownian's dynamics

Introduction

The aim of this work is the numerical modelling of the binding mechanism and the numerical evaluation of the association constant K_a as function of the relative distance between the Staphylococcal protein A (SpA) and the Fc regions. The SpA has received large interest in recent years, and it has been extensively studied in detail because of its high binding affinity towards antibody Fc domain.^[1,2] This protein contains a series of highly homologous IgG^[3] binding domains designated as A, B, C, D and E; all these domains can bind to the Fc portion of IgG. In this work, the analyses are focused on the fragment B of SpA because of its availability in complex with a human Fc fragment in a crystallized form. The comprehension of the involved kinetics is of noticeable interest for bio-sensing applications based on the

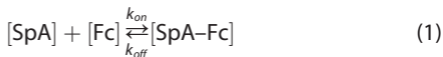
immobilization of antibodies on biosensor surface.^[4] The association constant is estimated from the analysis of the Brownian's trajectories calculated with the 'Simulation of Diffusional Association of proteins' code.^[5] The quantitative dependence of this parameter is taking into account with respect to the contact distance between SpA and Fc fragments. In particular, the residues, for all simulations, are all possible hydrogen bond donor-acceptor contact pairs^[5] formed between the SpA and Fc fragments within a distance of 6 Å.

Protein description

The molecular structures here considered are extracted from the X-ray crystallography data, PDB: 1FC2, available on the RCSB Protein Data Bank (PDB).^[6,7] The complex consists in a small portion of the protein A (domain B) and one-half Fc domain of the human IgG antibody. This system, shown in Fig. 1, is only a small portion of the whole SpA-IgG complex, but it includes the entire binding pocket relevant for the nonpolar and polar interactions.

Methods

The analysis is focused on the association between an immobilized capture reagent (B domain of protein A) and its target analyte (human IgG Fc fragment). The binding kinetics is described by the following 1 : 1 stoichiometric reaction:



The reaction rates k_{on} and k_{off} are obtained from the simulation of the Brownian's diffusional association of the two protein

fragments. The simulations of the association kinetics are performed taking into account a nonpolar term (directly proportional to the accessible surface area (653 \AA^2)^[9] of their nonpolar atoms) and electrostatic term. The Gibbs energy for the binding in this case is the sum of nonpolar and electrostatic (polar) contributions, and it is linked to the association constant as follows:

$$\Delta G^{binding} = \Delta G_{nonpolar}^{binding} + \Delta G_{electrostatic}^{binding} = -RT \ln(K_a \cdot [1M]) \quad (2)$$

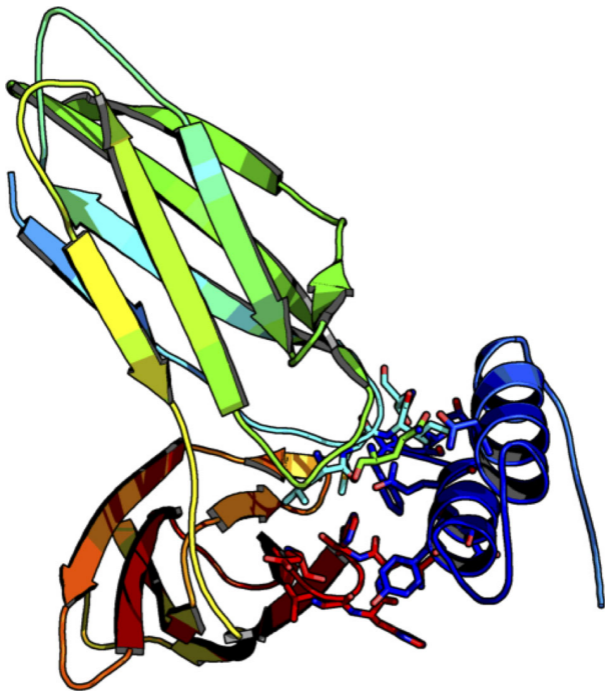


Figure 1. Cartoons and atomic model representation of the human Fc fragment and its complex with fragment B of protein A from 'Staphylococcus aureus' at 2.9-Å and 2.8-Å resolutions made by PyMol^[8] using the PDB structure 1FC2 from the RCSB Protein Data Bank. The green and red β -turns represent the Fc domain; in blue, the helices I and II cor-

responding to the B domain of protein A, and sticks are residues monitored during the simulation. The key residues for the interaction in the protein A is the hydrophobic region formed by Phe¹³² and Tyr¹³³ with polar and charged residues Asn¹²⁵, Lys¹²⁶, Gln¹²⁹, Asn¹³⁰, His¹³⁷, Glu¹⁴³, Arg¹⁴⁶, Asn¹⁴⁷ and Lys¹⁵⁴ around this region. In the Fc fragment, the residues Ile²⁵³ and Leu³¹⁴ give rise to the hydrophobic interaction. Other polar or charged residues Ser²⁵⁴, Gln³¹¹, Asp³¹⁵, Lys³¹⁷, Glu⁴³⁰, His⁴³³, Asn⁴³⁴ and His⁴³⁵ are located in the three β -turns at the interface.

The standard Gibbs energy change is obtained when $[SpA] = [Fc] = [SpA-Fc] = 1$ M. The protonation states for all simulations are determined employing the PDB2PQR Atomic charges and radii from the specified force fields^[10] AMBER99 and PROPKA pipelines to assign protonation states at different pH,^[11–13] and no energy minimization of the protein–protein complex is performed. The relative dielectric constant of water $\epsilon_s = 78.54$ and the solvent ionic strength $I_s = [25, 50, 75]$ mM ion concentration of Na⁺ and Cl[−] corresponding to a Debye–Hückel length $\lambda_{DH} = [19, 14, 11]$ Å. For the molecule region, $\epsilon_m = 2$, an infinite Debye length, and a simulation box equal to $[180 \times 180 \times 180]$ Å³ for the finest grid. Then, in order to define a successful binding of the structures in the 1FC2 complex, any pair of atoms in the binding pocket within a fixed pairwise distance of 6 Å is listed and subsequently screened during the simulations of $25 \cdot 10^3$ Brownian's trajectories. The results in Fig. 2 show the relative association constant, $K_a = k_{on}k_{off}^{-1}$.

Ionic strength dependence of the association constant

The binding process of the SpA–Fc complex shows a different behaviour compared to the description of a purely diffusion limited association process enhanced and driven by the protein–

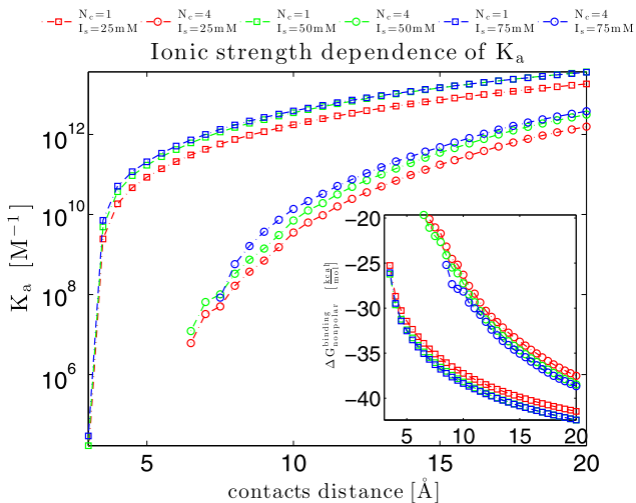


Figure 2. The plot shows the association constant K_a versus contact's distance, and the square symbols depict the behaviour according to a successful binding criterion with $N_c=1$ contact assuming three different ionic strength $I_s=75$ mM (blue), $I_s=50$ mM (green) and $I_s=25$ mM (red). The circles describe the behaviour according to a successful binding criterion with $N_c=4$ contacts with the same ionic strength previously defined. The subplot shows the electrostatic binding energy $\Delta G_{\text{nonpolar}}^{\text{binding}}$ versus contact's distance.

protein electrostatic interaction. The main reason of this difference is the nonpolar interaction between two helices of SpA and the Fc fragments of the IgG. In Fig. 2, the association constant K_a exhibited by the 1FC2 complex is not altered by the variation of the ionic strength. However, it is sensitive to the relative orientation between the SpA and Fc fragments.

In fact, due to the orientation constraints imposed specifying the minimum number of successful contacts $N_c=4$, the binding energy is $\Delta G_{\text{nonpolar}}^{\text{binding}} = -22$ kcal/mol less favourable compared to the value for $N_c=1$, $\Delta G_{\text{nonpolar}}^{\text{binding}} = -38$ kcal/mol both reached at pH=7 and 7 Å contacts distance. The association constant in the first case is reduced by few orders of magnitude depending on the contact distance (Fig. 2).

pH dependence of electrostatic binding energy and association constant

The effect of pH on the association constant between SpA–Fc fragments in the 1FC2 complex is also investigated. The electrostatic binding energy of the bound complex is computed for different pH values of the ionic environment. Looking to the net charges at pH=7, SpA and Fc fragments carry on $-5e$ and $+2e$, at pH=5 $-4e$ and $+10e$ and at pH=3, $+4e$ and $+28e$ charges. The Poisson–Boltzmann equation is solved using the adaptive finite difference method, and the electrostatic binding free energy is computed with the APBS numerical code.^[14] The binding electrostatic energy is the sum of the interaction and desolvation energy.^[15]

$$\Delta G_{\text{electrostatic}}^{\text{binding}} = \Delta G_{\text{electrostatic-int}}^{\text{binding}} + \Delta G_{\text{electrostatic-desol}}^{\text{binding}} \quad (3)$$

The binding electrostatic energy depends on the interaction among the charges of the Spa and Fc fragments. This value computed in the bound state is $\Delta G_{\text{electrostatic-int}}^{\text{binding}} = -1.67$ kcal/mol at pH=7. At pH=5, the electrostatic contribution $\Delta G_{\text{electrostatic-int}}^{\text{binding}} = -3.54$ kcal/mol is much more negative compared with the previous value. Solution at pH=3 dramatically changes the protonation states of the ionisable residues. In this case, all the charged residues in the binding pocket of the SpA and Fc fragments do not bear negative charges. These protonation states give rise to a non-negligible intermolecular electrostatic repulsive potential among positively charged residues Arg¹⁴⁶, His¹³⁷ and Lys¹⁵⁴ (Fig. 3), that are the sources of the unfavourable electrostatic binding energy $\Delta G_{\text{electrostatic-int}}^{\text{binding}} = 7.54$ kcal/mol. On the other side, the variation of the electrostatic desolvation binding energy $\Delta G_{\text{electrostatic-desol}}^{\text{binding}}$ among the solvent and SpA-Fc fragments is

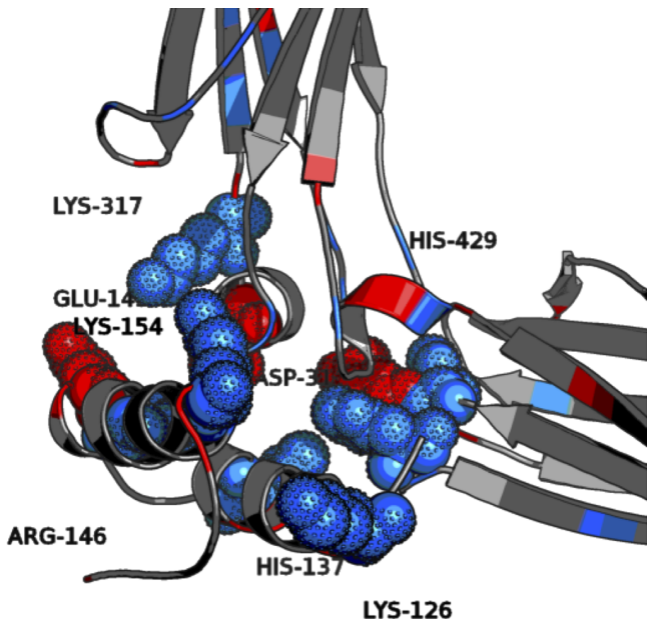
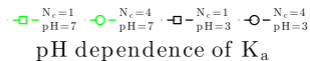


Figure 3. The residues are shown as dotted spheres and coloured according to their positive or negative charges in blue and red, respectively. 1FC2 rendered with PyMol.^[8]



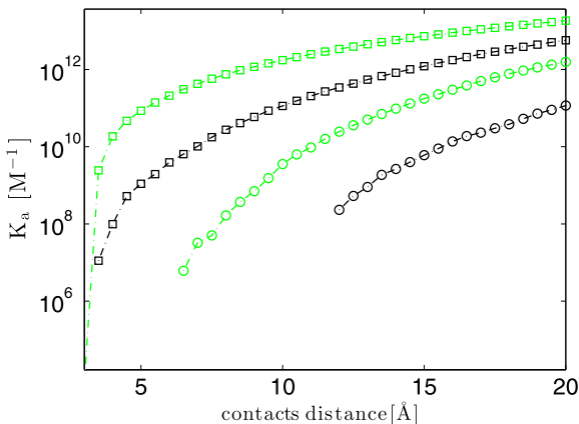


Figure 4. The plot shows the association constant K_a versus contact's distance, and the square symbols depict the behaviour according to a successful binding criterion with $N_c=1$ contact assuming a pH=7 in green and pH=3 in black. The circles depict the behaviour according to a successful binding criterion with $N_c=4$ contacts with the same pH previously defined.

unfavourable, to the binding process, for pH equal to 3, 5 and 7 upon binding. Hence, the behaviour of the association constant is modulated and remarkably dependent from the protonation states of few residues in the 1FC2 complex. It has been calculated the association constant for two values pH=3 and pH=7 (Fig. 4). Also in this case, the variation of the pH on the simulated statistical ensemble of Brownian's trajectories affects the association constant changing it approximately of two orders of magnitude. Subsequently, the closest contact distance between SpA and Fc fragments is influenced by the pH. For pH=3, the distance is

nearly 12 Å, that is, two times the distance reached at pH=7. Hence, low pH environment leads to a decrease in affinity of the SpA–Fc fragments due to their electrostatic repulsion.

Conclusions

The work presented here has analysed the effects of solvent ionic strength and pH variation on the association constant between SpA and Fc fragments. The same effects can be explained through the electrostatic energy too. For ionic strength ranging from 25 to 75 mM, the association constant between helices I and II of SpA and Fc is independent of the salt concentration. Moreover, K_a is sensitive to the relative orientation between the two proteins. This effect is highlighted by the different values of K_a obtained with different number of contacts observed at each specified distance for each pair of reaction atoms. In particular, for $N_c=1$, the complex SpA–Fc collides, whereas for $N_c=4$, the SpA–Fc fragments are tacitly steered in the correct direction.^[16] It has been also found that the pH affects the interactions in the binding pocket of SpA–Fc fragments by different mechanisms. At pH 5 or 7, the electrostatic interaction energy of the bound complex is favourable, and the association constants are much higher for every contact distance of the monitored residues if compared with the value obtained at pH=3 due to the unfavourable electrostatic interaction energy. In fact, the SpA and the Fc fragments both host neutral or positively charged residues due to the assigned protonation states at pH=3; as a consequence, all favourable electrostatic interactions among charged residues found at pH=5 and 7 are completely destroyed. Furthermore, the repulsion of certain residues in the SpA–Fc complex becomes the driving force for the unbinding mechanism.

Acknowledgement

This research was undertaken within the project EMRP HLT04, BioSurf. The EMRP participating countries within EURAMET and the European Union jointly fund the EMRP. The work was also supported by Progetto Premiale MIUR INRIM 'Metrology for therapeutic and diagnostic techniques based on electromagnetic radiation and ultrasound waves', (2014-2016).

References

- [1] K. Saha, F. Bender, E. Gizeli, *Anal. Chem.* **2003**, *75*, 835.
- [2] B. Huang, F.-F. Liu, X.-Y. Dong, Y. Sun, *J. Phys. Chem. B* **2012**, *116*, 424.
- [3] J. J. Langone, *Adv. Immunol.* **1982**, *32*, 157.
- [4] L. A. Clifton, C. Neylon, A. E. Terry, I. C. Dicko, I. A. Diddens, *Mater.Today* 2009, *12*, 86.
- [5] R. R. Gabdouliline, R. C. Wade, *Methods* 1998, *14*, 329.
- [6] D. Moiani, M. Salvalaglio, C. Cavallotti, A. Bujacz, I. Redzynia, G. Bujacz, F. Dinon, P. Pengo, G. Fassina, *J. Phys. Chem. B* 2009, *113*, 16268.
- [7] J. Deisenhofer, *Biochemistry* 1981, *20*, 2361.
- [8] W. L. Delano, *The PyMOL Molecular Graphics System*, DeLano Scientific, San Carlos, CA, USA, 2002.
- [9] D. Chakravarty, M. Guharoy, C. H. Robert, P. Chakrabarti, J. Janin, *Protein Sci.* 2013, *22*(10), 1453–1457.
- [10] J. Wang, P. Cieplak, P. A. Kollman, *J. Comput. Chem.* 2000, *21*, 1049.
- [11] T. J. Dolinsky, J. E. Nielsen, J. A. McCammon, N. A. Baker, *Nucleic Acids Res.* 2004, *32*, W665.
- [12] T. J. Dolinsky, P. Czodrowski, H. Li, J. E. Nielsen, J. H. Jensen, G. Klebe, N. A. Baker, *Nucleic Acids Res.* 2007, *35*, W522.
- [13] C. R. Søndergaard, M. H. M. Olsson, M. Rostkowski, J. H. Jensen, *J. Chem. Theor. Comput.* 2011, *7*, 2284.
- [14] N. A. Baker, D. Sept, S. Joseph, M. J. Holst, J. A. McCammon, *Proc. Natl.Acad. Sci.* 2001, *98*, 10037.
- [15] T. Wang, S. Tomic, R. R. Gabdouliline, R. C. Wade, *Biophys. J.* 2004, *87*, 1618.
- [16] S. H. Northrup, H. P. Erickson, *Proc. Natl. Acad. Sci.* 1992, *89*, 3338.